Towards A Unified Near-Field Intensity Map of the 2015 Gorkha, Nepal, Earthquake

Sujan Raj Adhikari,[a] Gopi Baysal,[a], Amod Dixit,[a] Stacey S. Martin,[b] Mattieu Landes,[c] Remy Bossu,[c] and Susan E. Hough[d]

We develop a unified near-field shaking intensity map for the 2015 Mw7.8 Gorkha, Nepal, earthquake by synthesizing intensities derived from macroseismic effects of the mainshock that were determined by independent groups using a variety of approaches.~~.~~ Independent assessments by different groups are generally consistent, with minor differences that are likely due in large part to differences in spatial sampling. Throughout most of the near-field region, ~~—~~European Macroseismic Scale (EMS-98) intensities were generally close to 7 EMS. In the Kathmandu valley intensities were ~~somewhat~~ slightly higher (6-7~~.5~~ EMS ~~–~~ 7-8 EMS~~.5~~) along the periphery of the valley and in the adjacent foothills than in the central valley, where they were ≈6 EMS. The results are consistent with instrumental intensity values estimated from available data using a published relationship between peak ground acceleration (PGA) and intensity. ~~—~~Using this relationship to convert intensities to PGA, we estimate strong-motion PGA deamplification factors of ≈0.7 in the central Kathmandu valley, with amplification of ≈1.6 in adjacent foothills. The results support the conclusion that the Kathmandu valley experienced a pervasively non-linear response during the Gorkha mainshock.

INTRODUCTION

While the 25 April 2015 M_W7.8 Gorkha, Nepal, earthquake caused a serious societal impact in Nepal in terms of loss of life and property, damage and fatalities were lower than experts had feared for an event of this magnitude~~,~~ in this location. Although there were instances of catastrophic collapse, overall damage was especially, and surprisingly, low within the Kathmandu valley, where only a small percentage of buildings sustained substantial to heavy damage. Studies have proposed this result to be due to long-period source radiation (*Galetzka et al.*, 2015), pervasive non-linear response within the Kathmandu valley *(Dixit et al*., 2015; *Bhattarai et al*., 2015; *Rajaure et al*., 2016), and the distribution of mainshock high frequency radiation (*Avouac et al., 2015; Hough et al*, 2016). There is thus an urgent need to better understand ground motions from the mainshock, and their implications for seismic hazard. Given that instrumental data are limited, it is further necessary to consider intensity data derived from macroseismic observations, which are expected to reflect relatively high frequency (≈1-5 Hz) ground motions (*Sokolov and Chernov*, 1998). In recognition of the importance of gathering macroseismic data, intensity and/or damage surveys were undertaken after the earthquake by a number of independent groups, using a number of different approaches including direct surveys of intensities using standard questionnaires (*Adhikari et al*., 2015; *this study*), direct surveys of building damage and other macroseismic effects (*Mencin et al.*, 2016; *Ohsumi et al.*, 2016), internet-based questionnaires (*Bossu et al.*, 2016), and the assessment of media accounts (*Martin et al.*, 2015; *McGowan et al*., 2016).). In this study we focus on the intensity distribution in the near-field region; outside of Nepal, the intensity distribution is constrained primarily by the results of *Martin et al.* (2015) as well as intensities determined from Web-based questionnaires (e.g., *Bossu et al*., 2016).

Formatted: Font: Italic

Of particular note, an extensive Building Damage Assessment (BDA) was conducted by the National Society for Earthquake Technology (NSET) with several international partner agencies under three projects that were supported by different donor agencies. A total of 291,891 individual buildings were assessed in the Kathmandu Valley and throughout the affected municipalities, to determine the observed damage grade according to 1998 European Macroseismic Scale guidelines (EMS-98; *Grunthal et al.*, 1998), and the building type. Using this database it is possible to determine the statistical incidence of damage grades for mud-brick masonry (assumed vulnerability Class A), cement-masonry (Class B), and reinforced concrete frame (Class C) structures at 847 individual locations within all municipalities impacted by the earthquake. We use these results to assign intensities using the EMS-98European Macroseismic Scale scale, hereinafter referred to simply as EMS-98 intensities.

To assess intensities reliably from media accounts, it is widely recognized that it is crucial to not give undue weight to isolated instances of damage, and to apply EMS-98 guidelines with an appreciation for issues associated with macroseismic effects of earthquakes in the Indian subcontinent (see *Martin & Hough*, 2016 for summary). Even when the same general guidelines are followed, intensity assessments from different approaches can differ due to either inherent subjectivity in interpretation of accounts (e.g., *Hough & Page*, 2011) or reliance on different types of information. *Hough & Pande* (2007) showed that media-based intensities for the 2001 Bhuj, India, earthquake were generally higher than intensities assigned from direct surveys (*Pande & Kayal*, 2003) of macroseismic effects. This discrepancy is consistent with a reporting bias whereby media reports are not necessarily over-dramatized per se, but are preferentially available from locations with relatively dramatic effects (e.g., *Bakun & Scotti*, 2006; *Hough*, 2013). As a first step towards synthesizing the results of independent studies, we compare the results from independent surveys to determine whether or not they are generally consistent.

We further use a relationship between peak ground acceleration (PGA) and EMS-98 intensity (*Worden et al.*, 2012; *Hough et al.*, 2016) to generate a map of PGA_{EMS} for the mainshock. We use this map to explore the amplification (and deamplification) of PGA within the Kathmandu valley.

INTENSITY RESULTS

We review briefly the independent intensity assessments considered in this study (Table 1; Figure 1). The NSET study was undertaken by a team of researchers beginning in May, 2015, using an intensity questionnaire that was formulated considering building types and local conditions in Nepal (*Adhikari et al.*, 2015; *Adhikari et al.*, 2016 *Murakami et al.*, 2016). Intensities were assigned for a total of 265 locations. These locations are concentrated in the Kathmandu valley, but sites outside the valley were surveyed as well. 2) The Nanyang Technological University (NTU) study was undertaken immediately following the mainshock, relying on detailed media accounts made available over the Internet, including photographs and CCTV footage, to determine EMS-98 values for 3,831 locations -within and outside of Nepal (*Martin et al.,* 2015). 3) The European Mediterranean Seismic Centre (EMSC) data set includes intensities determined automatically based on user-specified thumbnail illustrations corresponding to observed effects at different shaking levels (*Bossu et al*., 2016). 4) The University of Colorado, Boulder (CU) study was undertaken immediately following the earthquake, relying on assessment of EMS intensities based on direct inspection of damage and other effects, supplemented with assignments based on media accounts, at a total of 72 locations (*Mencin et al.*, 2016). 5) The DYFI-1 study includes 68 Modified Mercalli Intensity (MMI) values determined automatically from on-line questionnaires (see Wald *et al*., 1999). 6) The DYFI-2 study includes 16 near-field MMI values determined in one case from instrumental data and for 15 locations from assessment of media accounts (*McGowan et al*., 2016). Lastly, 7) the NSET-BDA study includes a total of over 800 intensity values determined from the exhaustive Building Damage Assessment project, which involved direct surveys of 291,891 individual buildings.

The NSET-BDA study far surpasses all of the other studies in both the number of individual locations surveyed and the rigor of damage assessments, providing the opportunity to assign EMS-98 intensities based on the observed statistical incidence of damage grades for different vulnerability classes. In effect, the availability of this extensive data set, which provides far more detailed information than is usually available for investigations of macroseismic effects, provides a unique opportunity to assess the veracity of the other studies, which represent more commonly used approaches to assess macroseismic intensity.

Table 1. List of Intensity surveys considered

Study.	Agencies	Approach	Locations
1	NSET	Direct questionnaire survey	265
2	NTU	Media-based	3,831
3	EMSC	Internet-based questionnaire	106
4	CU	Ground survey	72
5	DYFI-1	Internet-based questionnaire	68
6	DYFI-2	Media-based	16
7	NSET-BDA	Building Damage Assessment	291,891

Table 1 lists the approach used to assess intensities in each study. In some cases, more than one approach was used within the same study. The NTU study was overwhelmingly based on interpretation of media accounts from outside and within Nepal, with a small number of EMS-98 values based on both media accounts and available information from ground surveys. The CU study was primarily based on ground surveys, supplemented with a small number of intensities assessed from media accounts. Maps of intensity values from studies 1-6 are shown for the near-field region (Figure 1) and for the Kathmandu Valley (Figure 2), including the average and sample standard deviation for each data set.

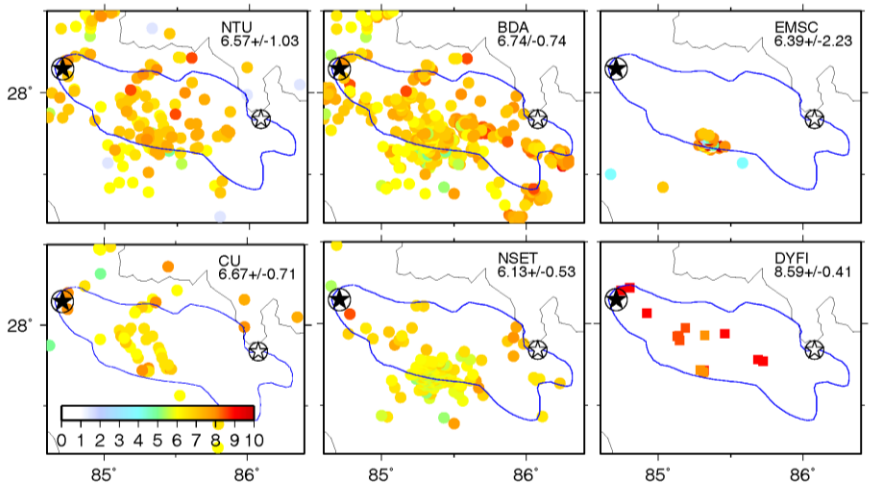

Figure 1. Intensity values throughout the near-field region from independent studies: CU (lower left), NSET (lower middle), DYFI-1 and DYFI-2 (lower right), NTU (upper left), BDA (upper middle), and EMSC values from individual questionnaires (upper right). In each panel, intensities are shown for individual locations (circles; color scale shown in lower left panel), which in some cases are averages from more than one questionnaire. The DYFI data include intensity values determined from online questionnaires and values determined from either instrumental data (one location) or from assessment of media accounts. Each panel also shows mainshock rupture (*Lindsey et al.*, 2015) (blue line), mainshock epicenter (black star), epicenter of 10 May 2015 Dolakha aftershock (white star), and average near-field intensity ± 1 σ shown for each dataset.

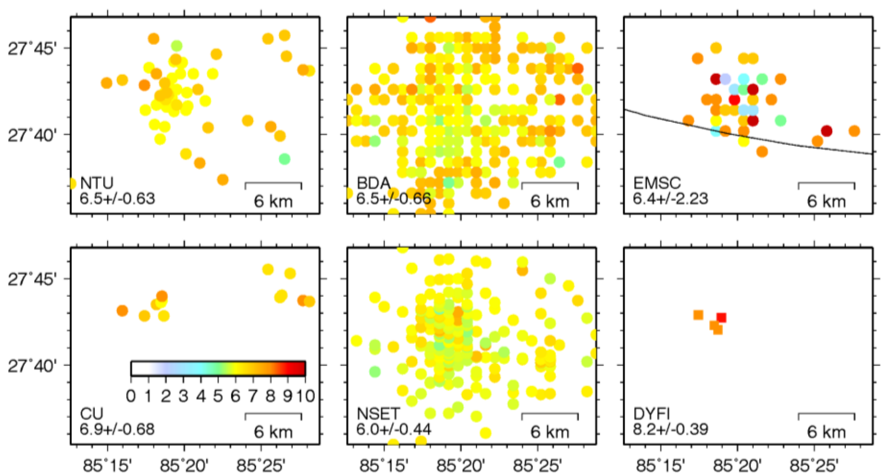

Figure 2. Intensity values in the Kathmandu Valley from independent studies: CU (lower left), NSET (lower middle), DYFI-1 and DYFI-2 (lower right), NTU (upper left), BDA (upper middle), and EMSC (upper right). In each panel, intensities are shown for individual locations (circles; color scale

shown in lower left panel), which in some cases are averages from more than one questionnaire. The DYFI data include intensity values determined from online questionnaires (circles) and values determined from either instrumental data (one location) or from assessment of media accounts (squares). Average near-field intensity ± 1σ shown for each dataset in each panel. Southern edge of mainshock rupture shown in top right panel from *Lindsey et al.* (2015) (dark line).

SYNTHESIS AND ANALYSIS OF DATA

Our initial comparison of the independent data sets (Figures 1 and 2) reveals that the NSET, BDA, NTU, EMSC, and CU studies are generally consistent to within ± 1 σ. The DYFI-1 data set includes few near-field values. DYFI-2 values, estimated subjectively from a limited number of media accounts (*McGowan et al.*, 2016), are higher than average intensities from other studies. Qualitatively, the difference between the DYFI-2 results and the other results are generally consistent with a reporting bias (e.g., *Bakun & Scotti*, 2004; *Hough and Pande*, 2007; *Hough*, 2014). While the NTU study was also based overwhelmingly on media accounts, the reporting bias appears to have been obviated by the exhaustive nature of the *Martin et al.* (2015) study, which involved a painstaking search of all available data sources including CCTV footage made available over the internet following the earthquake. *Martin et al.* (2015) further interpreted EMS-98 values with an appreciation for issues associated with assessment of intensities in the Indian sub-continent (see *Martin and Hough*, 2016).

Individual EMS-98 values from the EMSC study (*Bossu et al.*, 2016) reveal significantly more variability than any of the other studies. This variability likely reflects the nature of the data, which are derived from individual thumbnail questionnaire results with no spatial averaging, and without information about building type or vulnerability. Reports from individual locations with instances of catastrophic collapse would have been interpreted as high (9-10 EMS) intensity. Of note, however, the average raw intensity value across the Kathmandu valley is consistent with the average value from all of the other studies apart from DYFI-2. Since the DYFI-2 data set is both small and an outlier among the studies, we will not include it in our synthesis.

In light of the above considerations, our synthesis map for the Kathmandu Valley includes the NTU, EMSC, CU, DYFI-1, NSET, and BDA results. The small differences among the average intensities for these studies could reflect 1) systematic differences in subjective interpretation, 2) random scatter, or 3) sampling bias. Among these five studies, average intensity values across both the near-field and Kathmandu valley are consistent within ± 1 σ. It is reasonable to conclude that subjective interpretations were generally consistent among these studies, and consistent with the algorithms used for the EMSC and DYFI studies, and that differences result primarily from differences in sampling and/or spatial averaging. Furthermore, to the extent that there might have been differences in subjective interpretation, it is reasonable to average the results (e.g., *Hough and Page*, 2011). We therefore develop synthesis maps by combining the six intensity data sets, without attempting to calibrate individual intensity datasets. For the combined data set, we do omit several isolated 9-10 EMS values from the EMSC data set: because these intensities are point values, we expect that determination of a representative intensity for a given location will require averaging, which requires sufficient spatial sampling. In Figure 3 we present the combined intensity dataset for the Kathmandu valley. For the region defined by the map limits, the average EMS intensity is 6.4 ± 0.9.

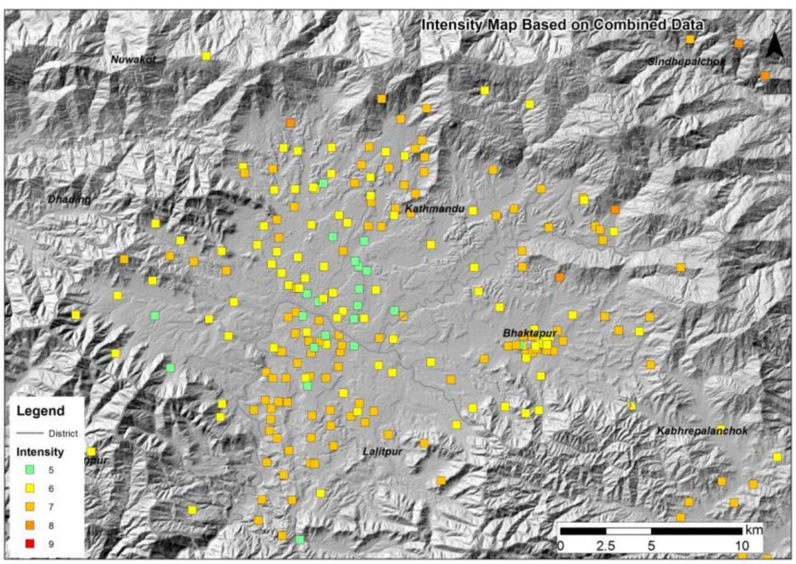

Figure 3. EMS intensity values throughout Kathmandu Valley, omitting EMSC values.

Figure 4 presents contoured EMS-98 intensities throughout the near-field region. To generate the interpolated map we use a Laplacian smoothing operator with a tension factor of

1.0, which ensures that no maxima or minima are generated except at control points (*Wessel & Smith*, 1999). To improve the visualization of the variability of EMS-98 values, in Figure 5 we show EMS-98 residuals throughout the near-field region, calculated by subtracting the near-field average of 6.6 from all values. (This average value is calculated using all intensities within 84.6-86.4W, 27.4-28.3N. Within the estimated rupture perimeter the average is ≈7 EMS).

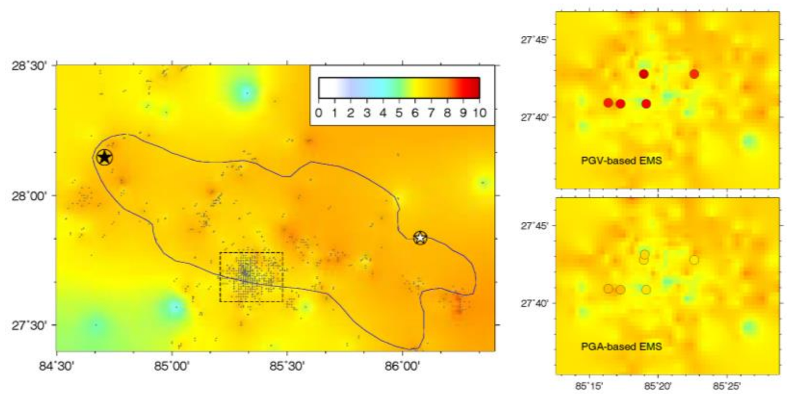

Figure 4a. (left) Contoured EMS-98 intensities (color scale indicated) across the near-field region; the mainshock rupture (*Lindsey et al.*, 2015) and Kathmandu Valley are shown with solid blue and dashed black lines, respectively. Small gray dots indicate locations where intensities are estimated. The intensity distribution in the northwest corner of the map, which is effectively unconstrained, is masked. 4b (right) Contoured intensities in Kathmandu valley (same color scale shown in Figure 4a). Filled circles in two panels indicate instrumental intensities estimated from PGA (bottom) and PGV (top).

Figures 3 and 4 reveal that EMS-98 values were overwhelmingly within a narrow range, 6 EMS to 7-8 EMS~~-7.5~~, throughout the Kathmandu valley as well as throughout the near-field region, reaching values as high as 8 EMS to 8-9 EMS~~-8.5~~ in only a few areas. This is consistent with the conclusions of earlier studies based on more limited datasets (*Martin et al.*, 2015; *Adhikari et al.*, 2016; *Mencin et al.*, 2016; *Hough et al.*, 2016). The spatial distribution of EMS-98 intensities in the Kathmandu valley is qualitatively similar to that observed in earlier studies, with the lowest values in the central, deepest part of the valley (Figure 3), and somewhat higher values around the periphery of the valley and in adjacent foothills. Figure 3 does not reveal any significant north-to-south trend across the Kathmandu valley; high residuals are observed in foothill locations in all directions with the possible except of the southwestern corner, where intensities are poorly constrained.

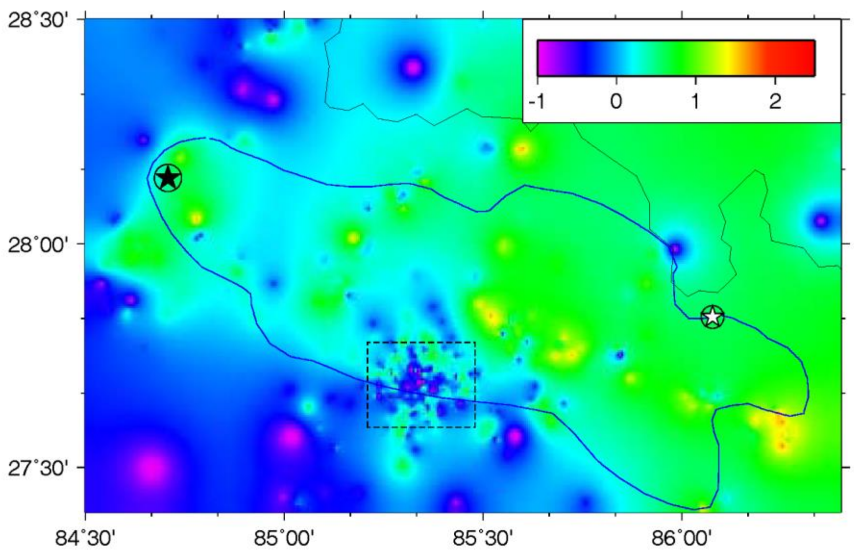

Figure 5. Contoured EMS-98 intensity residuals (color scale indicated) across the near-field region; the mainshock rupture (*Lindsey et al.*, 2015) and the Kathmandu valley are shown with solid blue and dashed black lines, respectively. The intensity distribution in the northwest corner of the map, which is effectively unconstrained, is masked.

The spatial distribution of intensities throughout the near-field region reveals some differences with the results of earlier studies (*Martin et al.*, 2015; *Hough et al.*, 2016). Consistent with the earlier studies, intensities are found to be generally higher towards the northern edge of the rupture, but unlike the earlier studies the swath of high intensities is less narrowly concentrated along the northern edge, instead revealing a swath of relatively high intensities close to the along-strike mid-line of the rupture. The average EMS-98 intensity across the near-field region is ≈7, slightly higher than that estimated by *Mencin et al.* (2016).

One can further consider the consistency of directly observed macroseismic data with limited instrumental recordings of the mainshock. Within the Kathmandu valley, available instrumental data include conventional strong motion recordings from a total of six sites (*Dixit et al.*, 2015; *Bhattarai et al.*, 2015; *Rajaure et al.*, 2016) as well as high-rate (5

Formatted: Font: Italic
Formatted: Font: Italic
Formatted: Font: Italic

samples per s) GPS from two sites (*Galetzka et al.*, 2015; also see *Hashash et al*., 2016). Stations KKN4 and KTP are hard-rock reference sites; TVU is a presumed thin-sediment site near the edge of the valley. The rest of the sites are within the valley. The GPS data provide no constraint on ground motions at frequencies above 2.5 Hz, and therefore peak ground acceleration (PGA), but do constrain peak ground velocity (PGV) (Table 2). Instrumental intensities, I_{PGA} and I_{PGV}, can be estimated from recorded PGA and PGV values using an intensity-prediction relationship; we use the relationships determined by Worden *et al.* (2012):

$$I_{PGA} = 1.78 + 1.55\log(PGA), \quad \log(PGA) \leq 1.57 \qquad (1)$$
$$I_{PGA} = -1.60 + 3.70\log(PGA), \quad \log(PGA) > 1.57$$

and

$$I_{PGV} = 3.78 + 1.47\log(PGV), \quad \log(PGV) \leq 0.53 \qquad (2)$$
$$I_{PGV} = 2.89 + 3.16\log(PGV), \quad \log(PGV) > 0.53$$

where PGA and PGV are in cm/s^2 and cm/s, respectively. The values are given in Table 2 and compared to observed intensities in Figure 4b.

Table 2. Instrumental Data from the Kathmandu Valley

STN	Latitude (°N)	Longitude (°E)	PGA (g)	I_{PGA}	PGV (cm/s)	I_{PGV}
KAT	27.713	85.316	16.5	6.6	107	9.3
DMG	27.719	85.317	17.8	6.7	--	--
KTP	27.682	85.273	24.6	7.2	52	8.3
TVU	27.681	85.288	24.2	7.2	99	9.2
PTN	27.681	85.319	15.4	6.5	74	8.8
THM	27.713	85.377	15.0	6.4	90	9.1
NAST	27.657	85.328	--	--	90	9.1
KKN4	27.801	85.279	--	--	70	8.7

Table 2. List of strong motion and high-rate GPS stations that recorded the Gorkha mainshock, including published PGA and PGV values (%g and cm/s, respectively), as well as I_{PGA} and I_{PGV} estimates from equations 1 and 2

As shown in Figure 4b, we find good consistency between I_{PGA} values and directly estimated intensities. Not only is the overall shaking level consistent; both estimated and directly estimated intensities reveal the same subtle difference between intensities in the valley versus the adjacent foothills. In contrast, I_{PGV} values are considerably higher than directly estimated intensities (Figure 4b, top). Intensities as high as 9 are grossly inconsistent with the low overall level of damage to highly vulnerable structures, revealing that the intensity-PGV relationship cannot explain ground motions within the Kathmandu valley during this earthquake.

To further explore the distribution of ground motions, we now use the *Worden et al.* (2012) relationships to estimate PGA_{EMS} (in cm/s^2) from estimated EMS intensities.

Although the *Worden et al.* (2012) relationship was developed using data from California, and using modified Mercalli intensity (MMI) rather than EMS-98, *Hough et al.* (2016) shows that it provides a good fit to available data from the Gorkha mainshock for PGA values above ≈1%*g*.

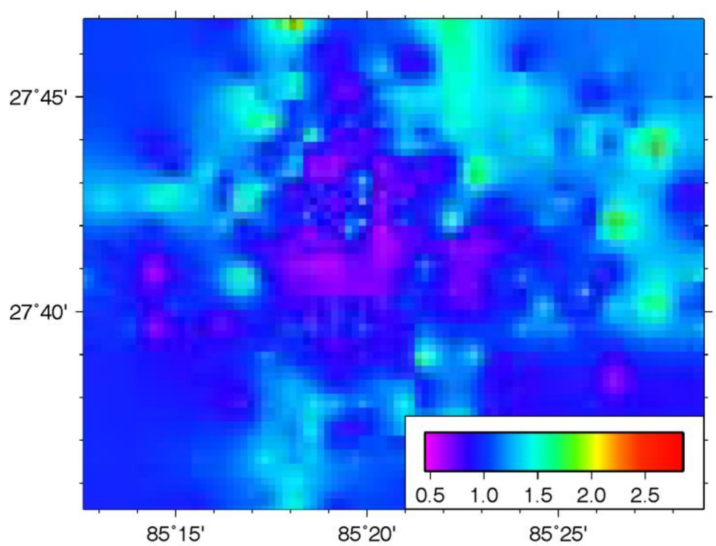

Figure 6. PGA residuals (amplification/deamplification factors) relative to the average, calculated by dividing estimated PGA_{EMS} values by the average across the the Kathmandu Valley.

Figure 6 shows estimated PGA_{EMS} amplification factors across the Kathmandu valley, estimated relative to the observed average, PGA_{AVE} (e.g., PGA_{EMS}/PGA_{AVE}). Estimated amplification factors are all in the range 0.4 – 4.5, with 93.6% between 0.5-2.9 (2.5% are below 0.5; 4.2% are above 2.9). The pattern of deamplification within the central Kathmandu valley, with modest amplification around the periphery of the valley and in the adjacent foothills, is clearly illuminated. Draping this result over topography (Figure 7) further illustrates this result. We note that residuals in the southwest corner of the region are effectively unconstrained.

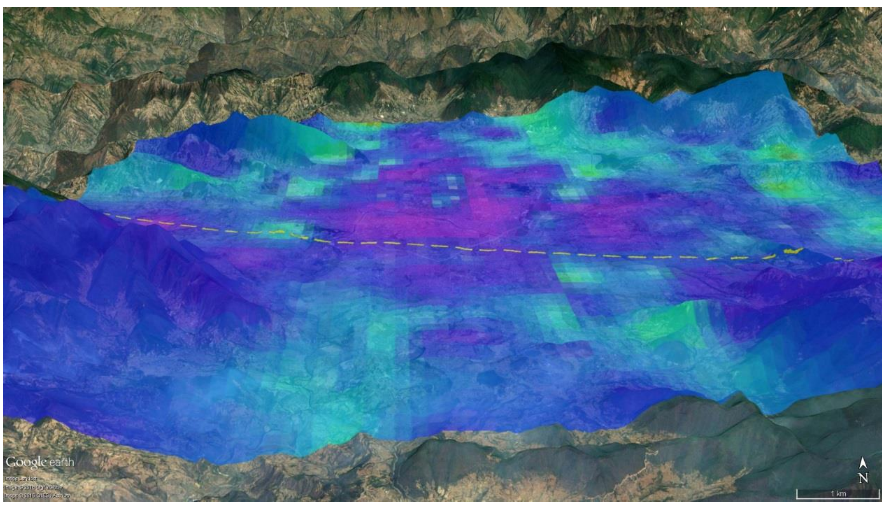

Figure 7. PGA residuals (amplification/deamplification factors; same color scale as shown in Figure 6.) from Figure 6 draped over topography (factor of 2 vertical acceleration) within the Kathmandu Valley. Dashed line indicates southern limit of mainshock rupture from *Lindsey et al.* (2015).

The amplification factors shown in Figure 7 are calculated relative to the average estimated PGA_{EMS} across the region rather than relative to directly estimated hard-rock reference values. Alternatively, one could divide all values by an average calculated for foothill sites only; however the results could be biased if, as suggested by Martin et al. (2015), topographic amplification was common. We note that this ambiguity is not unique to this study, and has likely been an unrecognized source of uncertainty in many past site response studies that relied on reference sites. We further note that *Rajaure et al.* (2016) estimated amplification factors of 0.60 – 0.92 directly from strong motion recordings of the mainshock from three sediment sites and one hard rock site. While the baseline used in this study might be open to question, are results are thus consistent with instrumentally constrained amplification factors.

DISCUSSION AND CONCLUSIONS

Given the limited instrumental recordings of the 2015 Gorkha mainshock, macroseismic data offers the best available information to constrain the distribution of near-field ground motions. In this study we compare and combine macroseismic data sets, including the extensive Building Damage Assessment, that were collected and interpreted by independent teams over the months following the mainshock. We find that assessment of EMS-98 intensities done by independent groups were generally consistent. The consistency of the media-based NTU results (*Martin et al.*, 2015) with results from direct surveys indicates that media-based intensity distributions can reliably capture representative shaking effects, if spatially rich macroseismic information is collected and carefully interpreted.

Directly estimated intensities are consistent with instrumental intensities estimated from available instrumental data in the Kathmandu valley using the intensity-PGA relationship developed by Worden *et al.* (2012), but inconsistent with instrumental intensities using the Worden et al. (2012) intensity-PGV relationship. I_{PGV} values are not plausible in light of the pervasively low level of damage to highly vulnerable structures in the Kathmandu valley, suggesting that, for this earthquake and this location, damage was controlled PGA rather than PGV. Two factors plausibly account for this result: 1) Vernacular structures in the valley, almost all of which are 1-4 stories, are not vulnerable to the longer period shaking that controlled PGV, such that high PGV values were not generally damaging, and 2) High-frequency energy levels and PGA were unusually low within the Kathmandu valley for reasons summarized in the following paragraph.

The combined EMS-98 data set provides improved spatial resolution of the distribution of ground motions during the Gorkha mainshock compared to early studies based on individual surveys. The distribution of near-field ground motions illuminated by this study confirms the earlier result that ground motions, and damage, within the central Kathmandu valley were lower than expected due to a pervasive non-linear response of valley sediments (*Dixit et al.*, 2015; *Bhattarai et al.*, 2015; *Rajaure et al.*, 2016; *Hough et al.*, 2016), with an estimated PGA deamplification factor of ≈0.7 in the central valley. While other factors, including source radiation and the distribution of high-frequency shaking might have also contributed to the relatively low shaking in the Kathmandu valley (e.g., *Avoauc et al.*, 2015; *Galetzka et al.*, 2015), it is clear from Figure 5 that shaking in the valley was significantly lower than other regions along the southern edge of the mainshock rupture. The deamplification factor within the central valley was sufficient to reduce EMS-98 intensities from 7+ to close to 6, a significant difference given the vulnerability of vernacular structures.

The overall distribution of near-field intensities reveals some similarities but also some differences from the distribution revealed by earlier studies (*Martin et al.*, 2015; *Hough et al.*, 2016). As in earlier studies (*Hough et al.*, 2016), we observe lower ground motions along the southern edge of the rupture, and higher shaking in the forward directivity direction. The swath of relatively high intensities, however, is less strongly concentrated along the far northern edge of the rupture, instead extending from the approximate north-south centerline of the rupture to its northern edge. We note, however, that the intensity distribution along the far northern edge of the rupture, along the southern edge of the high Himalaya, is poorly constrained (see Figure 4a). The improved intensity distribution will provide a useful constraint for future mainshock rupture modeling, as well as for development of shaking scenarios for future large earthquakes in the region

REFERENCES

Adhikari, S.R., Basyal, G.K., Pradhan, S and Shrestha, S. (2015), "Post-Earthquake Assessment Of Buildings Using Mobile Technology And Google Imaginary Plus GIS Visualization" 14th International Symposium on New Technology for Urban Safety of Mega Cities in Asia, Katmandu.

Adhikari, S.R., Guragain, R, and Murakami H. (2016), "Study on Shaking Intensity Distribution Of The 2015 Gorkha Earthquake In Nepal" international symposium on 1st anniversary of Gorkha earthquake,Nepal, DOI: 10.13140/RG.2.2.10485.78562.

Avouac, J-P., L. Meng, S. Wei, T. Wang, and J-P Ampuero (2015), Unzipping lower edge of locked Main Himalayan Thrust during the 2015, Mw7.8 Gorkha earthquake, *Nature Geoscience*, **8**, p. 708 – 711,doi:10.1038/ngeo2518.

Bakun, W.H. and Scotti (2006). Regional intensity attenuation models for France and the estimation of magnitude and location of historical earthquakes, Geophyical Journal International, 164 (3), 596-610, *doi: 10.1111/j.1365-246X.2005.02808.x*

Bhattarai, M., L. B. Adhikari, U. P. Gautam, A. Laurendeau, C. Labonne, R. Hoste-Colomer, O. Sèbe, B. Hernandez (2015). Overview of the Large 25 April 2015 Gorkha, Nepal, Earthquake from Accelerometric Perspectives, *Seism. Res. Lett.* **86,** 6, DOI: 10.1785/0220150140

Bossu, R., R. Landès, F. Roussel R. Steed, R. Mazet-Roux, S.S. Martin, and S.E. Hough (2016). Thumbnail-Based Questionnaires for the Rapid and Efficient Collection of Macroseismic Data from Global Earthquakes, *Seism. Res. Lett.*

Dixit, A.M., A. Ringler, D. Sumy, E. Cochran, S.E. Hough, S.S. Martin, S. Gibbons, J. Luetgert, J. Galetzka, S.N. Shrestha, S. Rajaure, and D. McNamara (2015), Strong motion recordings of the M7.8 Gorkha, Nepal, earthquake sequence from low-cost, Quake Catcher Network accelerometers, *Seismological Research Letters*, **86**, 6, p. 1533 – 1539, doi: 10.1785/0220150146.

Galetzka, J., D. Melgar, J.F. Genrich, J. Geng, S. Owen, E.O. Lindsey, X. Xu, Y. Bock, J-P. Avouac, L-B. Adhikari, B.N. Upreti, B. Pratt-Sitaula, T.N. Bhattarai, B. Sitaula, A. Moore, K.W. Hudnut, W. Szeliga, J. Normandeau, M. Fend, M. Flouzat, L. Bollinger, P. Shreshta, B. Koirala, U. Gautam, M. Bhatterai, R. Gupta, T. Kandel, C. Timsina, S.N. Sapkota, S. Rajaure, N. Maharjan (2015). Slip pulse and resonance of Kathmandu basin during the 2015 Mw7.8 Gorkha earthquake, Nepal, imaged with space geodesy, *Science*

Grünthal, G., R.M.W. Musson, J. Schwartz and M. Stucchi (eds.) (1998), The European Macroseismic Scale EMS-98, Conseil de l'Europe, Cahiers du Centre Europeén de Geodynamique et de Seismoligie, Luxembourg, **15**, p. 101.

Hashash, Youssef MA, Binod Tiwari, Robb ES Moss, Domniki Asimaki, Kevin B. Clahan, D. Scott Kieffer, Doug S. Dreger et al. "Geotechnical field reconnaissance: Gorkha (Nepal) earthquake of April 25, 2015 and related shaking sequence." *Geotechnical Extreme Event Reconnaisance GEER Association Report No. GEER-040* (2015): 1-250.

Hough, S.E. (2013), Spatial Variability of "Did You Feel It?" Intensity Data: Insights into Sampling Biases in Historical Earthquake Intensity Distributions, *Bulletin of the Seismological Society of America*, **103**, 5, 2767–2781, doi:10.1785/0120120285.

Hough, S.E. and P. Pande (2007), The 1868 Hayward Fault, California, Earthquake: Implications for Earthquake Scaling Relations on Partially Creeping Faults, *Bull. Seism. Soc. Am.*, **97**, p. 638 – 645, doi:10.1785/0120060072.

Hough, S. E., and M. Page (2011), Toward a consistent model for strain accrual and release for the New Madrid Seismic Zone, central United States, *Journal of Geophysical Research – Solid Earth*, **116**, B3, 2156-2202, doi:10.1029/2010JB007783.

Hough, S.E., S.S. Martin, V.K. Gahalaut, A. Joshi, M. Landès, & R. Bossu (2016), A Comparison of Observed and Predicted ground motions from the 2015 Mw 7.8 Gorkha, Nepal, Earthquake, *Natural Hazards*, **84**, 1661-1684, doi:10.1007/s11069-016-2505-8.

Lindsey, E.O., R. Natsuaki, X. Xu, M. Shimada, M. Hashimoto, D. Melgar, and D.T. Sandwell (2015). Line-of-sight displacement from ALOS-2 interferometry: Mw7.8 Gorkha earthquake and Mw7.3 aftershock,*Geophys. Res. Lett.*, **42:16**, 6655-6661. doi:10.1002/2015GL065385.

Martin, S.S., S.E. Hough, and C. Hung, 2015. Ground motions from the 2015 Mw7.8 Gorkha, Nepal, earthquake constrained by a detailed assessment of macroseismic data, Seism. Res. Lett., 86:6, 1524-1532, doi:10.1785/0220150138.

Martin, S.S. and S.E. Hough, 2016. Reply to "Comment on 'Ground Motions from the 2015 Mw 7.8 Gorkha, Nepal, Earthquake Constrained by a Detailed Assessment of Macroseismic Data' by Stacey Martin, Susan E. Hough and Charleen Hung" by Andrea Tertulliani, Laura Graziani, Corrado Castellano, Alessandra Maramai, and Antonio Rossi, Seism. Res. Lett. 87:4, 957-962, doi:10.1785/0220160061.

McGowan, S.M., K.S. Jaiswal and D.J. Wald (2016). Using structural damage statistics to derive macroseismic intensity within the Kathmandu valley for the 2015 M7.8 Gorkha, Nepal earthquake, Tectonophysics.

Mencin, D., Bendick, R., Upreti, B.N., Adhikari, D.P., Gajurel, A.P., Bhattarai, R.R., Shrestha, H.R., Bhattarai, T.N., Manandhar, N., Galetzka, J. and Knappe, E., 2016. Himalayan strain reservoir inferred from limited afterslip following the Gorkha earthquake. *Nature Geoscience*, 9, 533-537, doi:10.1038/ngeo2734.

Murakami, H., R. Gurgain, S.R. Adhikari, G. Basyal and S. Mori (2015). Seismic intensity questionnaire survey for the 2015 Gorkha, Nepal earthquake – Preliminary results and damage observations. Japan Association of Earthquake Engineering.

Ohsumi, T., I. Hiroshi, H. Inoue, S. Aoi, and H. Fujiwara (2016). Investigation of damage in and around Kathmandu Valley related to the 2015 Gorkha, Nepal earthquake, Technical Note of the National Research Institute for Earth Science and Disaster Prevention, 404, 53 pp

Pande, P., and J. R. Kayal (eds.) (2003), Kutch (Bhuj) Earthquake 26 January 2001, Geological Survey of India, Special Publication **76**, Lucknow.

Rajaure, S., D. Asimaki, E. Thompson, S.E. Hough, P. Ampuero, S.S. Martin, A. Inbal, and M. Dhital, Strong motion observations of the Kathmandu valley response during the M7.8 Gorkha earthquake sequence, *Tectonophysics, doi: 10.1016/j.tecto.2016.09.030*.

Sokolov, Y. Yu, and Yu. K. Chernov (1998). On the correlation of seismic intensity with Fourier Amplitude Spectra, Earthquake Spectra, 14 (4), 679-694.

Wald, D. J., V. Quitoriano, L. Dengler, and J. W. Dewey (1999), Utilization of the Internet for Rapid Community Intensity Maps, *Seism. Res. Lett.*, **70**, 6, p. 680 – 697,doi: 10.1785/gssrl.70.6.680.

Wessel, P., and W.H.F. Smith (1999), Free software helps map and display data, *Eos Transactions*, AGU, **72**, p. 441 – 445,doi: 10.1029/90EO00319.

Worden, C.B., M. C. Gerstenberger, D. A. Rhoades, and D. J. Wald (2012), "Probabilistic Relationships between Ground-Motion Parameters and Modified Mercalli Intensity in California,*Bulletin of the Seismological Society of America*, **102**, p. 204 – 221, doi: 10.1785/0120110156.